DOI: 10.13009/EUCASS2019-314

Ideal Geometries and Potential Benefit of Variable Pitot Inlets for Subsonic and Supersonic Business Aviation

Stefan Kazula, Mark Wöllner, David Grasselt, and Klaus Höschler
Brandenburg University of Technology Cottbus-Senftenberg
Siemens-Halske-Ring 14, 03046 Cottbus, Germany

Abstract

The challenge of determining ideal inlet geometries for variable pitot aero engine inlets in transonic and supersonic civil aviation is presented. The trade-off in inlet design and the geometric inlet parameters are introduced. By means of a parametric design study, feasible inlet geometries for variable inlets are identified and the potential aerodynamic benefit of using variable pitot inlets for flight speeds from Mach 0.95, 1.3 up to 1.6 is examined. After considering the additional weight of variable inlets, for instance due to required actuators, a remaining range benefit of over 20% at a flight speed of Mach 1.6 is determined.

1. Introduction

The aviation industry is constantly striving to improve efficiency, reduce emissions and increase travel speed, while ensuring safety and reliability [1]. One way to achieve these goals is to improve aero engines and their integration into the aircraft. Currently, aero engine inlets are designed as a rigid trade-off concerning aerodynamic requirements at different subsonic flight conditions. Many studies concerning inlets are dealing with the aerodynamic design of the ideal trade-off geometry [2], [3], [4], [5], [6].

However, applying variable inlets instead of rigid trade-off inlets could further reduce the drag and thereby enable increased efficiency and flight speed [7]. Although research studies [8], [9], [10], [11] concerning circular variable inlets with adjustable lip and duct geometry for subsonic civil aviation were conducted, this technology has not made its way into service yet. An explanation for not implementing variable inlets in subsonic aviation may also be the low benefit in this range of speeds, as the minor benefit in aerodynamic efficiency may not compensate for the increased complexity and weight [12]. Variable inlets for transonic or even supersonic applications could have a higher potential for improvements than those for subsonic aviation. Furthermore, several aircraft manufacturers are conducting research on ambitious programs concerning supersonic business jets for the future [13], [14]. The only commercial supersonic applications have been the Tupolev Tu-144 and the Concorde, both being retired. These aircraft types utilised two-dimensional non-circular inlets with variable ramps and bypass flaps to adjust the inlet geometry and to prevent engine surge. Due to their rectangular geometry, very long inlets were required to attenuate inlet distortion. This length and the required actuation system for the ramps resulted in high additional weight.

Compared to a two-dimensional inlet geometry, an axisymmetric circular pitot inlet provides air of higher uniformity to the compressor system, enabling a shorter design, and thus less weight as well as better integration into the aircraft. However, only few researchers, e.g. Slater [15], have addressed the possibility of utilising supersonic pitot inlets, as other inlet types provide higher efficiency, described via the pressure recovery ratio. While axisymmetric circular pitot inlets produce high losses at flight Mach numbers above 2.0, they can be utilised up to Mach 1.6 with an acceptable pressure recovery ratio of 90 % [16], [17].

It has to be considered that the ideal lip and duct geometry of a pitot inlet for supersonic operation differs from that of a subsonic pitot inlet. The ideal geometry for supersonic flight conditions would result in an increased susceptibility towards flow separation due to crosswind and large angles of incidence during take-off and climb conditions up to Mach 0.3. By implementing a variable inlet geometry, it is possible to avoid flow separation during take-off and climb, while ensuring maximum efficiency during cruise flight.

Moreover, in 14 CFR Part 91.817 the Federal Aviation Administration (FAA) prohibits the operation of civil aircraft at flight Mach numbers greater than 1.0 over land, mostly for reasons of excessive noise generation due to sonic boom [18]. Therefore, a potential commercial supersonic aircraft may fly with a speed of Mach 0.95 over land and of

DOI: 10.13009/EUCASS2019-314

Mach 1.6 over sea to comply with these regulations. Thus, a variable inlet should be able to adjust the ideal geometry for subsonic cruise over land and for supersonic cruise over sea, as well as a tolerable geometry for take-off and climb conditions.
Knowledge of the ideal geometry for these flight phases is necessary to develop and evaluate concepts for feasible variable pitot inlets. Therefore, the challenge of determining the ideal inlet geometries within a preliminary concept study for circular variable aero engine inlets in transonic and supersonic civil aviation [19], [20], [21], [22], [23] is presented. First, the trade-off in inlet design and aerodynamic evaluation criteria of inlets for different Mach numbers are introduced. Subsequently, the utilised process of the parametric design study and its implementation are described. The ideal inlet geometries for subsonic and supersonic cruise flight conditions are identified and compared to a modern industrial inlet, which represents the trade-off in design of rigid inlets. This way, the aerodynamic benefit of using variable pitot inlets is determined; and thereby, the potential of this technology is identified.

2. Aero engine inlets

2.1 Tasks

An aircraft requires lift and thrust to fly. The lift is generated by the air flow around the wings and the thrust by the aero engines. To produce thrust, an aero engine requires air, which is provided by the nacelle inlet, also called intake. The primary objective of the inlet is to divide the free stream in front of the aero engine at the stagnation point into an internal and an external air flow. The ratio of internal to external air flow depends on the operating conditions. The external air flow shall stream along the outer nacelle surface, while avoiding flow separation and minimising aerodynamic drag [24]. The internal air flow must provide the aero engine with the correct quantity of air at a desired flow velocity and uniformity during each operating condition, while minimising aerodynamic losses [25].
Depending on flight speed and operating conditions, the required air mass flow varies, resulting in different capture streamtubes. The capture streamtube is a model to describe the correlation between the area of undisturbed freestream air in front of the engine that flows into the engine A_0 and the inlet entry Area A_1. Although the stagnation point and the inlet entry area vary depending on the operating conditions, the highlight area of the inlet approximately represents the entry area A_1 for cruise flight conditions. From the highlight area to the engine throat area A_{th}, the duct for the internal flow decreases in diameter. Choking or blockage of the inlet due to compressible effects is avoided for this case by limiting the radially averaged Mach number in the engine throat Ma_{th} to values of 0.7 to 0.8 [24], [17]. This way, the amount of air mass flow required by the engine is ensured [17]. The axial flow velocity required by the aero engine's compressor system Ma_2 is in the range of Mach 0.4 to 0.7 [26] and commonly implemented around Mach 0.5 [27]. Therefore, at flight speeds above Mach 0.5, a deceleration of the internal air flow is necessary to ensure a highly efficient and safe operation of the compressor system. For this reason, the inner geometry of the inlet duct is designed as a diffuser [17], compare Figure 1.
The uniformity of the air flow influences the efficiency and the operational stability of the compressor system. Therefore, flow separations of the internal air flow should be avoided under all conditions, as they can lead to vibration excitation, rotating stall and engine surge. Engine surge results in reduced aero engine durability and a loss of thrust. A loss of thrust can cause hazardous events during certain flight phases when multiple engines are affected [28].

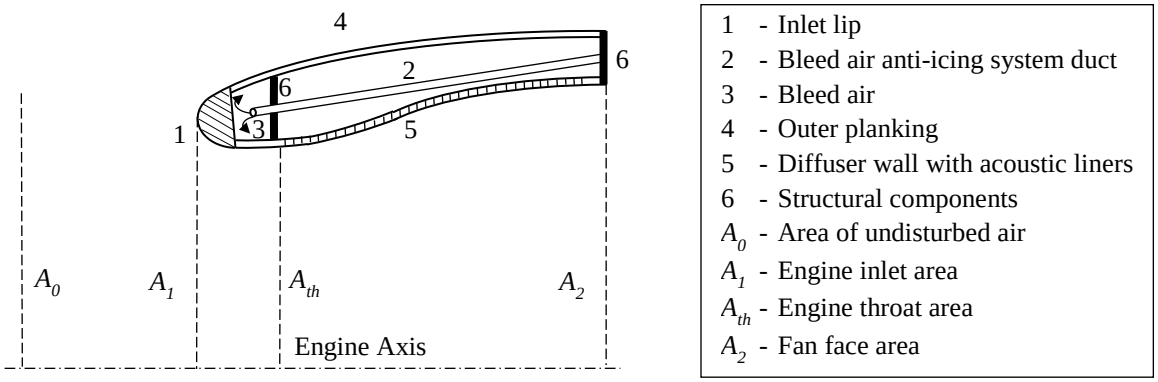

Figure 1: Typical design of a rigid subsonic inlet

DOI: 10.13009/EUCASS2019-314

2.2 Trade-off in design

During the geometric design of inlets, different requirements have to be satisfied to ensure reliable operation, while achieving high efficiency [16]. These requirements lead to contrary design solutions. On the one hand, it is necessary to avoid flow separations and potentially resulting hazardous events during take-off and climb operation up to Mach 0.3. On the other hand, the inlet should be highly efficient during cruise operation at high flight velocities above Mach 0.8.
High efficiency at high subsonic flight velocities can be achieved by a thin lip contour combined with a small entry area A_1 to minimise drag [17]. Also, a longer diffuser can be required to avoid flow separations when the entry area is reduced [2], [29]. Pitot inlets can be used for flight Mach numbers up to 1.6 without significant losses [16], [17]. At these supersonic regimes, a sharp inlet lip with a smaller entry area that matches the required air flow is more suitable to minimise the detachment of the normal shock in front of the inlet. This way, resulting losses, e.g. due to spillage drag, can be reduced [16], [15].
At low aircraft velocities during take-off and climb, where high angles of incidence and crosswind can occur, a sharp or thin lip contour is susceptible to flow separation and its potential negative consequences [30]. A round and thick inlet lip with a large inlet area is ideal for these operating conditions [30]. However, such a 'blunt' lip geometry causes higher drag, and thus reduced efficiency during operation at higher flight Mach numbers [30].
Hence, conventional rigid inlets can only accomplish a geometry that provides a trade-off concerning minimum drag at high velocities and avoidance of flow separation at low velocities. This results in increased drag at high flight velocities compared to an ideal contour for these operating conditions. The complex and challenging task of determining the most suitable trade-off geometry for subsonic applications has been investigated in numerous research studies [2], [3], [4] and [6]. Nevertheless, the limitations of conventional rigid inlets can be circumvented better by using variable pitot inlets, which adjust the ideal inlet geometry for each flight condition. As a result, efficiency can be improved, and maximum flight speed can be increased up to Mach 1.6, while flow separations are avoided. Although research studies concerning circular variable inlets with adjustable lip and duct geometry have been conducted, e.g. [8], [11] and [10], none of these inlets are yet in service in commercial aviation.
A potential reason is that these studies focus on subsonic operation, where limited efficiency gains are expectable. The small expectable advantages of the improved aerodynamics could be eliminated or even negated by the additional weight and the higher complexity of the variable design. Hence, supersonic applications up to flight speeds of Mach 1.6 are investigated in this study. However, the exact aerodynamic potential of supersonic pitot inlets must be identified by determining and analysing the ideal geometries for the expected operating conditions.

2.3 Inlet evaluation criteria

The performance of an aero engine inlet is primarily evaluated by its achieved pressure recovery, provided flow uniformity and produced external drag [16], [17].
The pressure recovery of the inlet influences the amount of thrust that an engine can provide. Hereby, 1 % loss of pressure recovery is equal to 1 % up to 1.5 % loss of thrust [16]. At high-speed flight, the inlet converts the free stream air in front of the aero engine to an internal air flow of a lower Mach number and a higher static pressure to satisfy the requirements of the engine. Thereby, the free stream total pressure p_{t0} is reduced to a value p_{t2} at the fan face due to losses. These losses of total pressure can be caused by surface friction, turbulent mixing in association with flow separation, and compressible effects, e.g. shock waves [16]. The pressure recovery ratio of p_{t2} to p_{t0} is commonly used to describe the efficiency of an inlet [16]:

$$\pi_{inl} = \frac{p_{t2}}{p_{t0}}. \tag{1}$$

For subsonic conditions, pressure recovery values of pitot inlets are higher than 0.90 at low flight speeds and can increase with flight speed up to 0.99 [16], [30]. At supersonic flight speeds, the pressure recovery value decreases to a theoretical maximum of $\pi_{inl} = 0.98$ at Mach 1.3, $\pi_{inl} = 0.90$ at Mach 1.6, and $\pi_{inl} = 0.72$ at Mach 2 [16] due to the total pressure loss from the single normal shock that results from using a pitot inlet at supersonic conditions.
Flow uniformity at the fan face is necessary to avoid vibration excitations and flow separations, which can lead to engine surge or flame out, resulting in loss of thrust and reduced lifetime [31], [32]. Therefore, the air, delivered by the inlet to the engine, shall be axially directed and uniform in velocity, temperature, as well as pressure [16]. The uniformity of the air flow at the fan face A_2 can be influenced negatively by high angles of attack, high angles of incidence, crosswind and the inlet design [16]. At cruise conditions, flow separation due to unsuitable inlet design is the main reason for low quality flow uniformity.

DOI: 10.13009/EUCASS2019-314

The external nacelle front drag $D_{nacf,ext}$ mainly depends on the inlet design and comprises the pre-entry drag D_{pre} and the cowl forebody drag D_{fb}, see Figure 2. While the inlet represents the outer nacelle surface from the inlet lip stagnation point area A_1 to the plane of the fan face A_2, and hence only a share of the forebody, the forebody drag still mainly depends on the inlet design. However, the whole nacelle up to the area of the maximum diameter A_{max} has to be considered during inlet drag investigations, as changes of the inlet design have a large impact on the static pressure distribution on the outer nacelle surface between A_2 and A_{max}.

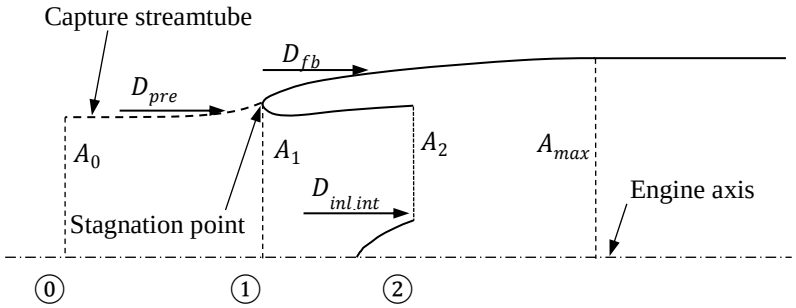

Figure 2: Components of inlet drag

The pre-entry drag D_{pre}, also known as additive drag, is a force that is defined by the integral of the difference between static pressure p_{ext} and ambient pressure p_0 over the capture streamtube [16], [17], [24], [30], [33]:

$$D_{pre} = \int_{A_0}^{A_1} (p_{ext} - p_0) dA. \tag{2}$$

The cowl forebody drag D_{fb} is the sum of the pressure drag and the friction drag over the forebody. The forebody describes the region between the inlet lip stagnation point area A_1 and the area of the maximum outer nacelle diameter A_{max}:

$$D_{fb} = \int_{A_1}^{A_{max}} (p_{ext} - p_0) dA + \int_{A_1}^{A_{max}} \tau dA\,. \tag{3}$$

The first term of this equation represents the axial pressure drag, which arises from the difference of the static pressure over the outer nacelle surface projected in the direction of the flow p_{ext} and the static ambient pressure p_0. The second term describes the friction drag resulting from the viscous shear stresses τ in the boundary layer of the nacelle forebody surface. Depending on the inlet design, the static pressure over the outer nacelle can be lower than the ambient pressure at subsonic cruise, as the flow is accelerated around the inlet lip and continues to flow with an increased velocity along the forebody. Hence, in this case a suction force can arise, which is also called lip suction force [17] or cowl thrust force [16]. For subsonic cases, where a difference between pre-entry drag and forebody drag exists, this difference is referred to as spillage drag [17]. At supersonic conditions, the static pressure p_{ext} is increased due to the normal shock in front of the engine. This additional drag due to compressibility effect is also referred to as wave drag [34]. The increased pressure after a shock requires a sharp and thin geometry to avoid further shocks and to minimise the projected area of the inlet lip and the forebody.

3. Approach

The utilised process to determine ideal inlet geometries concerning range at Mach 0.95, 1.3 and 1.6 is displayed in Figure 3. The first step to achieve the ideal geometries is the development of an aerodynamic model. The second step is the identification of the ideal geometries by means of an optimisation. The goal of this approach is to roughly identify ideal dimension tendencies of the inlet system. Hence, a detailed manipulation of curve parameters, as for example required for the generation of a constant velocity profile is unnecessary. Those investigations have been conducted, for instance by Albert [4], [5], Schnell [6] and Kulfan [35].

DOI: 10.13009/EUCASS2019-314

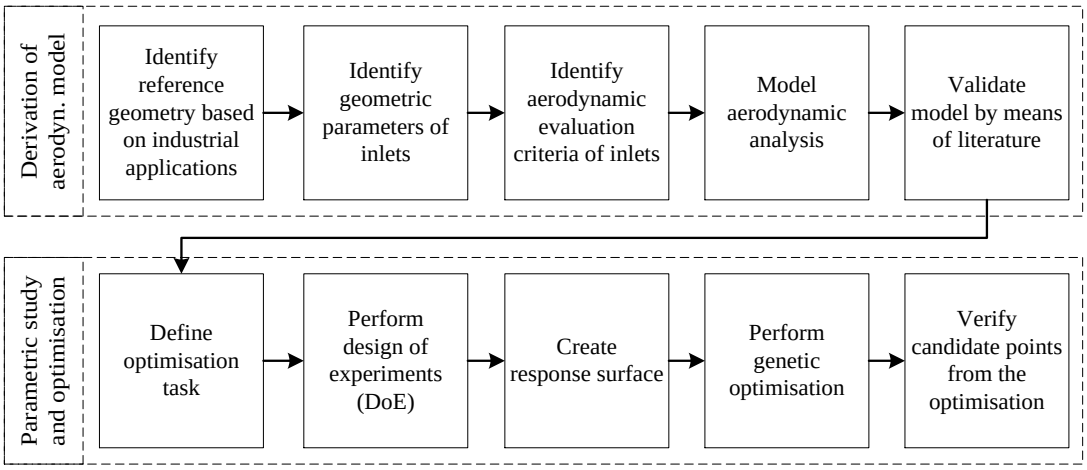

Figure 3: Process of the parametric design study to determine ideal inlet geometries

The most suitable geometry for each flight condition shall be implemented by the kinematic system of the variable inlet. Variable inlets must satisfy many requirements, e.g. concerning weight, kinematic feasibility, design space and complexity. These requirements result in constraints, e.g. concerning lip thickness, inlet entry radius or inlet length. Therefore, the ideal geometry concerning drag is not necessarily the most suitable to be implemented.
For instance, a long diffuser would result in a heavy inlet system. Thus, three different cases for length adjustment are examined in this study. Figure 4a, and b presents options, where the variable inlet has a fixed length, while its other parameters, e.g. throat diameter and lip aspect ratio, are adjustable. The length of the first option is based on an operational proven reference geometry that meets the industrial trade-off in inlet design and is applicable during take-off. The second option uses a longer inlet for all flight conditions. Figure 4c introduces an option that adjusts the inlet length from the reference geometry for take-off to longer inlets for cruise conditions. However, knowledge of an reference geometry, which is in service, is necessary in the first place.

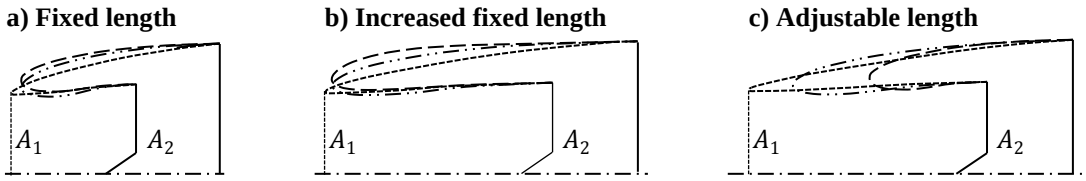

Figure 4: Options for the geometry adjustment of a variable inlet system

3.1 Reference geometry and parametrisation

Utilising a freely created geometry as reference would lead to significant relative improvements in a subsequent optimisation. Instead, it has been decided to derive the reference geometry from an inlet in service to achieve more realistic results. A simplified Rolls-Royce Pearl 15 engine inlet [36] has been selected as template [37], as it belongs to the most modern engines for civil business aviation, which is the primary area of application for variable pitot inlets. This engine is utilised in business jets like the Bombardier Global 6500, which is designed for cruise speeds of Mach 0.85 and top speeds of Mach 0.9 [38]. The diameter of the fan d_2 has been set to 1.28 m and the maximum nacelle diameter d_{max} to 1.86 m [39].
Improving efficiency and increasing travel speed can be achieved by improvements of the implemented cruise geometry. At cruise flight conditions, the occurring angles of inflow incidence and crosswind are usually negligible. Therefore, the ideal inlet geometry for that condition is approximately axisymmetric. Hence, the derived inlet reference geometry, as well as all other inlet geometries in this study, are simplified to an axisymmetric inlet, although real pitot inlets have different cross-sections for optimised operation, noise emission and accessory integration [5].
The inlet reference geometry has been converted into a parameterised Siemens NX12-sketch, see Figure 5. All contour splines are tangentially linked to each other. The fan diameter d_2, the maximum nacelle diameter d_{max}, the concatenated areas, as well as the inlet cone geometry are fixed.

DOI: 10.13009/EUCASS2019-314

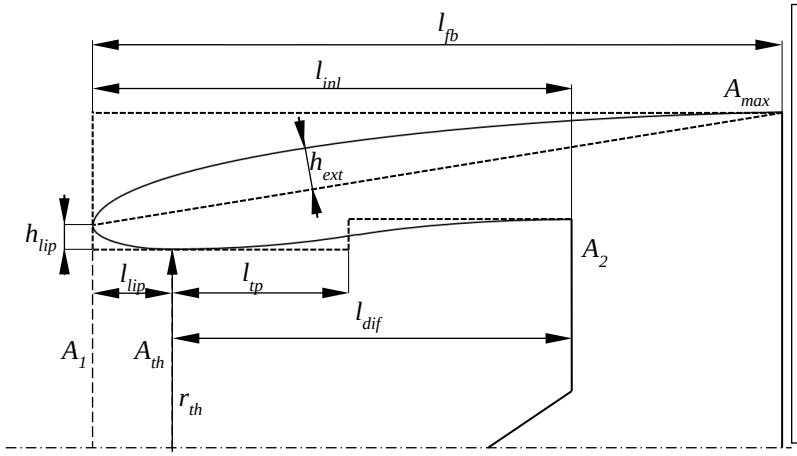

A_{max}	-	Maximum nacelle area
A_1	-	Engine inlet area
A_{th}	-	Engine throat area
A_2	-	Fan face area
h_{lip}	-	Lip height
h_{ext}	-	Nacelle forebody height
l_{fb}	-	Nacelle forebody length
l_{inl}	-	Inlet length
l_{dif}	-	Diffuser length
l_{tp}	-	Throat-turning point distance
l_{lip}	-	Lip length
r_{th}	-	Engine throat radius

Figure 5: Inlet parametrisation

The parameterised sketch is used to examine the influence of geometric parameters on the inlet drag and losses, as well as the provided mass flow quantity and the occurrence of flow separation at subsonic and supersonic flight conditions by means of a flow analysis. The geometric parameters, which are utilised to investigate the influence on the inlet evaluation criteria during the optimisation, are

- The inlet length l_{inl}, comprising the diffuser length l_{dif} and the lip length l_{lip},
- The radial lip height h_{lip} and length l_{lip}, which contribute to the lip fineness ratio l_{lip}/h_{lip} [2],
- The inlet throat radius r_{th}, which contributes to the lip contraction ratio $\left(r_{th} + h_{lip}\right)^2/(r_{th})^2$ [2] and
- The forebody height h_{ext} that describes the curvature and thickness of the external contour.

3.2 Modelling of the aerodynamic analysis

The aerodynamic analysis has been modelled and conducted in Ansys Fluent 18. The analysis is 2D axisymmetric, what allows for significantly reduced computational efforts. The atmospheric data have been taken from Military Handbook 310 [40]. A relevant mean cruise altitude of 14 km is represented through the Gulfstream G650ER business aircraft [41]. A Mach number of $Ma_2 = 0.5$ at the fan face and a pressure recovery of $\pi_{inl} = 0{,}99$ have been stipulated [17], [26], [16]. Additionally, an adiabatic friction-free shock has been assumed for the supersonic cases [30]. By means of the equations for ideal gases, isentropic processes and Bernoulli's principle, the boundary conditions have been determined and validated by means of literature [30], [42], [43].
A structured bisected C-grid has been chosen, as it is most suitable to reproduce the flow field near the curved inlet lip [44]. Additionally, a high boundary layer resolution of the nacelle walls is important to detect potential flow separations and to determine the inlet drag [45], [46]. A suitable boundary layer solution for these tasks is ensured by dimensionless wall distance values of $y^+ < 1$ [45], [47].
In the two-dimensional axisymmetric flow simulation, the Reynolds-averaged Navier-Stokes (RANS) equations for mass, momentum and energy conservation are iteratively solved for every node of the generated mesh in only two spatial directions, axial and radial [48], [49]. The RANS model enables acceptable computational costs and accuracy. Additionally, the k-ω-SST turbulence model has been selected, as it provides an acceptable prediction of the separation behaviour of a boundary layer from smooth surfaces even in combination with reversed pressure gradients and shocks [48], [50], [49]. The solving of the differential equation system comprising the RANS and turbulence model equations for fast compressible flows with eventual shocks is preferably conducted by a density-based method [51]. Additionally, a 2nd-order-upwind-discretisation of the differential equations has been chosen to achieve reduced numerical discretisation errors. The node based Green-Gauss algorithm has been used to determine the required gradients of differential equations, as it represents the most accurate method for this task [49]. Furthermore, the solving has been conducted implicitly, offering stable convergence properties combined with fast solving speed, while requiring increased memory [49]. This increased memory requirement has been acceptable due to the relatively small grid of less than a million nodes in conjunction with the utilised 32GB RAM system [51].
It is necessary to validate the model, as it is based on simplifications and boundary condition assumptions. While experimental tests provide a very high certainty for the correctness of the simulation results, a validation by means of validated models in literature is more time and cost efficient, while being suitable for this preliminary investigation. Hence, the boundary conditions [52], [30] and results from the introduced model [15], [53] have been compared with literature and show good agreement in all cases [37].

DOI: 10.13009/EUCASS2019-314

3.3 Optimisation task

The goal of this optimisation is to minimise the external drag $D_{nacf,ext}$ of inlet geometries for different flight conditions depending on the geometric design variables $\boldsymbol{x}_G$, while providing uniform air flow at a constant total pressure recovery:

$$\min_{\boldsymbol{x}\in X} D_{nacf,ext}(\boldsymbol{x}_G)\,. \tag{4}$$

Design variables $\boldsymbol{x}$ are the parameters that are varied during the optimisation [54]. The design space X also includes lower $\boldsymbol{x}^l$ and upper constraints $\boldsymbol{x}^u$ for the design variables:

$$X = \{\boldsymbol{x} \in \mathbb{R}^7 |\, \boldsymbol{x}^l \leq \boldsymbol{x} \leq \boldsymbol{x}^u\}\,. \tag{5}$$

In the present study, the design variables are categorised in geometric $\boldsymbol{x}_G$ and aerodynamic design variables $\boldsymbol{x}_A$:

$$\boldsymbol{x} = [\boldsymbol{x}_G^T, \boldsymbol{x}_A^T]^T \tag{6}$$

with

$$\boldsymbol{x}_G = \left[l_{dif}, l_{lip}/h_{lip}\,, h_{ext}, h_{lip}\,, r_{th}\right]^T \tag{7}$$

and

$$\boldsymbol{x}_A = [Ma_{th}, \tau_W]^T \tag{8}$$

The constraints of the geometric design variables $\boldsymbol{x}_G$ are presented in Table 1. The lip height and ratio are chosen to be fixed for the supersonic investigation, as these values represent parameters for minimum achievable drag, while ensuring that the design remains feasible for variable inlets. The inlet length l_{inl} should be limited to 200 % of the reference value, as a longer inlet could lead to uneconomically high weight. Thereby, diffuser length l_{dif} and lip length l_{lip} are also constrained. Furthermore, additional optimisations with different values for the maximum diffuser length l_{dif} have been conducted to determine ideal geometries for the different kinematic options that are shown in Figure 4.

Table 1: Geometric constraints for inlet geometries

Geometric parameter		**Reference value**	**Subsonic flight**		**Supersonic flight**	
			Lower constraint	*Upper constraint*	*Lower constraint*	*Upper constraint*
Diffuser length	l_{dif} [mm]	600	600	1388	750	1623
Lip ratio	l_{lip}/h_{lip} [-]	2.77	1.00	4.00	1.00	1.00
Nacelle forebody height	h_{ext} [mm]	98	28	120	28	120
Lip height	h_{lip} [mm]	78	20	80	10	10
Engine throat radius	r_{th} [mm]	586	550	620	550	620

The constraints of the aerodynamic design variables $\boldsymbol{x}_A$ are represented by the fluid shear stress value τ_W, which must be higher than 0 to exclude cases, where flow separation occurs, as well as by the throat Mach numbers Ma_{th} that should not exceed values of 0.75 to avoid losses due to shock waves.

3.4 Response surface optimisation

The Design of Experiments (DoE) method has been applied to generate response surfaces, which have been utilised to conduct the optimisation efficiently. The DoE is a method for determining an ideal design point distribution in the design space X by utilising Optimal Space-Filling (OSF) [55]. The OSF is a Latin Hypercube Sampling (LHS) algorithm with subsequent optimisation. The LHS generates a design point distribution, where no parameter values of design points are identical. The subsequent optimisation provides an ideal design point distribution by maximising the distance between them [55].

DOI: 10.13009/EUCASS2019-314

The present study utilises 100 design points for the variation of the geometric design variables, representing a relatively high design space resolution and accuracy. For each of the 100 design points, an automated mesh generation, initialisation and solving has been performed.
By means of a regression analysis, response surfaces have been generated from the results of the 100 DoE design points. This way, the correlations between input and output parameters have been determined [55]. The regression analysis leads to a small systemic error, which is negligible during this preliminary investigation.
The identification of the ideal design point in the defined design space has been achieved by using a genetic optimisation with elitism approach [56]. In the present study, 10.000 design points have been chosen as initial population size. The external drag of the randomised design points of the initial population is approximated by means of the response surface. This enables the application of an indirect optimisation instead of a direct optimisation, which would require 10.000 complete simulations, resulting in high computational efforts [56], [55]. For all cases of the present study, the optimum has been identified after 10 to 20 iterations, which have been conducted in 2 minutes.
As the optimisation is based on the response surface, the identified candidate points and the best design points from earlier iterations have been simulated thoroughly to proof the predicted drag value and to verify that the optimum has been determined.

4. Results

4.1 Selection of ideal geometries for variable inlets

The tendencies of aerodynamically ideal values of the geometric parameters for the given constraints are presented in Table 2. For flight speeds of Mach 1.3 and 1.6, only small differences in behaviour of the aerodynamic drag have been monitored for all geometric parameters in the investigated intervals. Thus, it is reasonable to summarise the according tendencies to a common supersonic case. This also leads to a reduced complexity of the variable pitot inlet system, as the same geometry is realised for all supersonic flight cases up to Mach 1.6. However, the identified tendencies are largely depending on the selected boundary conditions, e.g. deviations from the assumed engine mass air flow would lead to changes of the capture streamtube and result in new ideal geometries.

Table 2: Tendencies of ideal geometric parameter values for inlet geometries

Geometric parameter		Subsonic up to Mach 0.95	Supersonic up to Mach 1.6
Diffuser length	l_{dif}	Maximal	Maximal
Lip ratio	l_{lip}/h_{lip}	> 3	1
Nacelle forebody height	h_{ext}	High	Low
Lip height	h_{lip}	High	Low
Engine throat radius	r_{th}	> 560	580..620

For subsonic flight at Mach 0.95, long inlets with long diffuser lengths l_{dif} are aerodynamically preferable, as they lead to long forebodies, which can achieve the highest suction force [37], [57]. Supersonic designs achieve the lowest drag for long inlets, and hence long forebodies, as the curvature of the external geometry decreases, and this way, the projected axial pressure [37], [57]. Flow separation on the inner inlet surface is avoided in both cases, due to smaller diffuser divergence angles θ_{dif}. Moreover, the longer the inlet, the better distortions can be compensated [58].
For the subsonic case, a lip ratio l_{lip}/h_{lip} that is greater than 3.0 avoids high maximum throat Mach numbers and flow separations on the lip surface [37], [57]. Ideal lips for supersonic pitot inlets are sharp and thin [15], hence the lip ratio was set to 1.0 in combination with a low lip height h_{lip} of 10 mm. These values achieve relatively low drag, while avoiding flow separation and enable manufacturable and reliable designs. Additionally, these lips are less prone to flow separation than sharp lips in case of unsuitable capture streamtubes, large angles of incidence or crosswind.
Within the design space, large lip heights h_{lip} are desirable for subsonic cruise flight [37], [57]. Although these greater lip heights lead to increased pre-entry drag D_{pre}, the simultaneous reduction of the forebody drag D_{fb} is dominating [37], [57].
The curvature at the front of the external nacelle surface, which is represented by the nacelle forebody height h_{ext}, should be relatively high for subsonic cases, as it correlates with a higher resulting suction force on the forebody [37], [57]. At supersonic flight conditions, a high curvature leads to additional shock-induced losses on the external surface, while no curvature results in high losses at the transition from the forebody to the region of the maximum nacelle diameter. Therefore, a small forebody curvature is preferable during supersonic operation with a value of 56 mm resulting from the optimisation.

DOI: 10.13009/EUCASS2019-314

In relation to the inlet length, the engine throat radius r_{th} has a small influence on the drag for subsonic conditions. However, a throat radius of at least 560 mm should be selected to ensure high inlet total pressure recovery and to avoid flow disturbances. For the investigated supersonic conditions, throat radii in the range of 580 to 620 mm provided good solutions that avoided flow disturbances on the inner inlet surface, as well as on the outer forebody surface [37], [57].

Table 3 presents the determined geometric parameters that the variable inlet system shall realise. For all subsonic flight conditions, a single geometry is chosen for the variable inlet system. This applies respectively for the supersonic geometry that is selected for all flight Mach numbers greater than 1.0. This way, the variable inlet system must set only two different geometries and the complexity of variable inlet concepts can be minimised.

Table 3: Selected parameter values for variable inlet geometries

Geometric parameter		Reference	Subsonic up to Mach 0.95	Supersonic up to Mach 1.6
Diffuser length	l_{dif} [mm]	600	1388	1623
Lip ratio	l_{lip}/h_{lip} [-]	2.8	3.5	1.0
Nacelle forebody height	h_{ext} [mm]	98	112	56
Lip height	h_{lip} [mm]	78	70	10
Engine throat radius	r_{th} [mm]	586	560	620

Although the geometry for subsonic cruise flight at Mach 0.95 has not been simulated or tested for take-off and climb conditions, it is reasonable that it is suitable for these conditions as well. The chosen lip ratio and the lip length are increased compared to the reference. Thus, the incoming air flow has relatively more time to adapt to the flow direction of the inlet. Furthermore, the optimised subsonic geometry is longer than the reference. This results in smaller diffuser divergence angles that are less prone to flow separation. The flow around the forebody is also improved, as the forebody length is increased, and thereby its curvature is decreased. Moreover, for all aircraft speeds, the throat radius of 560 mm leads to theoretical average throat Mach numbers of less than 0.7 [30], which is acceptable [37], [57]. This average Mach number results in reduced shocks and boundary disturbances. However, take-off, climb and windmilling conditions must be investigated during subsequent, more detailed phases of the variable inlet development process.

The diffuser lengths l_{dif} for subsonic and supersonic operation are chosen in a way that allows for a constant length l_{inl} of the variable inlet. Without the need for greater length adjustments, the variable inlet can be designed less complex. This way, more robust and reliable concepts can be developed.

For design reasons, it is very desirable to have a fixed highlight radius r_1. This fixed radius enables the utilisation of inlet concepts with a circumferential rigid lip. Compared to concepts with circumferential segmented inlet lips [22], [59], such an unsegmented lip is expected to be much more resilient to potentially occurring external loads like birdstrikes. Hence, a fixed highlight radius r_1 must be chosen that is suitable for subsonic and supersonic conditions, see Figure 6. The highlight radius r_1 results from the engine throat radius r_{th} and the lip height h_{lip}. A value of 630 mm represents a suitable trade-off for the highlight radius r_1. On the one hand, it allows for a high lip height, while achieving the minimal throat radius for subsonic conditions. On the other hand, the resulting engine throat radius for supersonic conditions does not lead to flow separation on the forebody surface [37], [57].

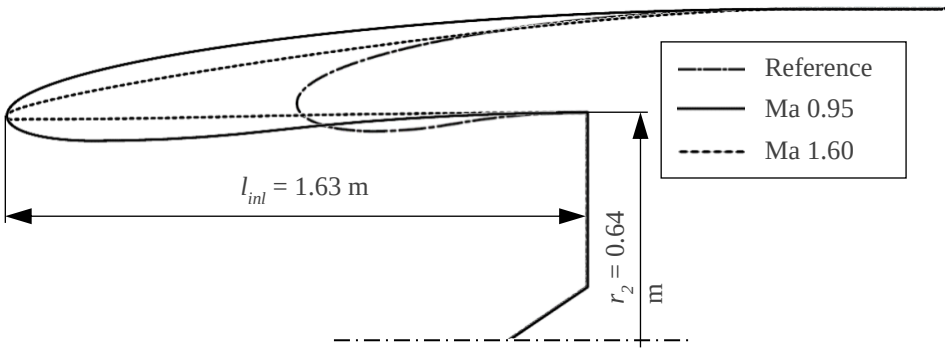

Figure 6 Ideal inlet geometries of variable inlets at Mach 0.95 and Mach 1.6

The selected geometries have been identified according to the results from the response surface optimisation. Hence, it is necessary to verify them by means of respective simulations to ensure their feasibility at the relevant operating conditions, see Figure 7.

DOI: 10.13009/EUCASS2019-314

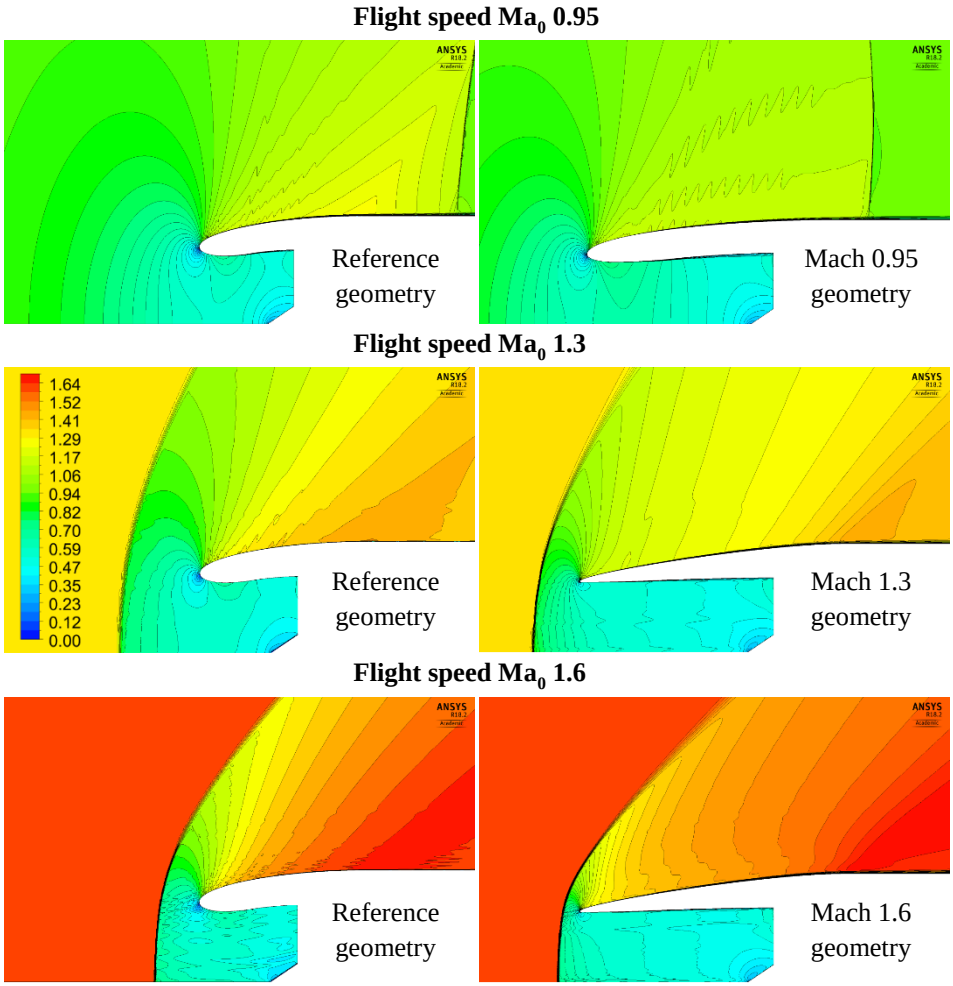

Figure 7: Mach number distribution of the reference geometry (left) and the selected geometries (right) at Mach 0.95, 1.3 and 1.6 (same scale for every plot)

These simulations reveal that the new geometries achieve improved flow patterns and lead to lower drag than the reference geometry that is designed for flight at Mach 0.85. At a flight speed of Mach 0.95, the supersonic area around the forebody has a smaller extension and the maximum occurring Mach numbers are lower for the optimised geometry. While the optimised geometry achieves over 700 N less drag for flight at Mach 0.95, the reference geometry remains more efficient by 50 N for its design point at Mach 0.85.

For the supersonic cases, the normal shock in front of the inlet is less detached from the lip for the optimised geometry, resulting in reduced spillage drag. Furthermore, the extension and the angle of the normal shock are smaller. This indicates an attenuated shock, what is confirmed by the higher occurring Mach numbers downstream of the shock.

The verification of the candidate geometries by means of detailed simulations reveals that a significant drag reduction compared to the reference geometry is achieved for all considered flight speeds, see Table 4. The increased inlet length proves to be the dominant geometric parameter for inlet drag reduction, as the optimisation with fixed reference length achieves only negligible drag improvements of up to 11%.

Table 4: Performance of the selected ideal geometries for a variable inlet at different flight speeds

Evaluation criterion		**Subsonic**	**Supersonic**	
		Mach 0.95	*Mach 1.3*	*Mach 1.6*
Pre-entry drag	D_{pre} [N]	1360	2750	4100
Forebody drag	D_{fb} [N]	-1340	3450	6520
External nacelle front drag	$D_{nacf,ext}$ [N]	20	6200	10620
Drag difference to reference	ΔD [N]	740	4580	9080
Pressure recovery	π_{inl} [-]	0.993	0.977	0.893

DOI: 10.13009/EUCASS2019-314

The application of the subsonic geometry optimised for Mach 0.95 at flight speeds of Mach 1.6 leads to a drag value $D_{nacf,ext}$ of 15660 N and the utilisation of the supersonic geometry for Mach 1.6 at flight speeds of Mach 0.95 results in a value of 800 N, demonstrating the necessity of variable pitot inlets for efficient transonic or supersonic transport.

4.2 Potential benefit of variable inlets

While current business jet can maintain maximum operational cruise speeds of Mach 0.90 to 0.925 [38], [41], this speed causes high drag and is compensated at cost of increased fuel consumption, and thus less range. Variable inlets allow for decreased drag at these and even higher flight Mach numbers. This way, they contribute to a reduction of the required fuel amount m_{fuel} and an increase of payload and range R. The benefit of variable inlets concerning required fuel and achievable range can be determined by means of the Breguet range equation [30]:

$$R = \frac{c_0}{g \cdot SFC} \cdot \frac{F_L}{F_D} ln\left[\frac{m_{to,max}}{m_{to,max} - m_{fuel}}\right] . \tag{9}$$

The flight range R is hereby dependent on the flight speed c_0, the maximum take-off weight of the aircraft $m_{to,max}$, the weight of the carried fuel m_B, the aircraft drag force F_D, the aircraft lift force F_L, the thrust specific fuel consumption SFC, as well as the gravitational acceleration g.
A reduction of the aircraft drag force F_D can be achieved by utilising variable inlets that decrease the external nacelle front drag $D_{nacf,ext}$. This applies under the assumption that the remaining aircraft drag is not negatively affected by the variable inlet. Under the condition that flight speed, gravity and specific fuel consumption are constant and with the simplification that lift force, maximum take-off weight and fuel weight remain approximately unchanged when utilising variable inlets, the flight range R is only depending on the aircraft drag F_D:

$$R \sim \frac{1}{F_D} . \tag{10}$$

This allows for the determination of the range increase of an aircraft with a number n of engines that utilise variable inlets R_{vinlet} compared to a reference aircraft without variable inlets R_{ref}:

$$R_{vinlet} = R_{ref} \cdot \frac{F_{D,ref}}{F_{D,ref} - n \cdot \Delta D_{nacf,ext}} . \tag{11}$$

Furthermore, the reduction of aircraft drag leads to a decreased fuel consumption $\dot{m}_{fuel}$, and hence less required fuel weight for a fixed flight range. This also allows for a greater payload to be carried by the aircraft, improving its economic performance. The approximation of the natural logarithm from Equation (9) for the relevant range of weights [30] results in:

$$\dot{m}_{fuel} \sim \frac{1}{R} \sim F_D \tag{12}$$

and

$$\dot{m}_{fuel,vinlet} = \dot{m}_{fuel,ref} \cdot \frac{F_{D,ref} + n \cdot \Delta D_{nacf,ext}}{F_{D,ref}} . \tag{13}$$

The drag $F_{D,ref}$ of a reference aircraft can be determined by means of the air density ρ, the flight velocity c_0, the characteristic area A and the drag coefficient c_D:

$$F_D = \frac{1}{2} \cdot \rho \cdot {c_0}^2 \cdot c_D \cdot A . \tag{14}$$

The air density ρ at a business jet relevant flight altitude of about 14.000 m can be derived from the barometric formula. The flight velocity c_0 can be calculated from the Mach number and the speed of sound at flight altitude considering occurring temperatures. Moreover, these values can be taken from literature [40]. The drag coefficient c_D is highly depending on the aircraft geometry, the choice of characteristic area and the flight Mach number. For

DOI: 10.13009/EUCASS2019-314

subsonic flight above Mach numbers of 0.7, values around 0.025 and for supersonic flight up to Mach 1.6, values of about 0.035 can be found [60], [61]. Wing area, frontal area or surface area of the aircraft can be selected as characteristic area [62]. These values can also be found in literature, e.g. [34]. For this example, the wing surface of the Gulfstream G650 of about 120 m² has been chosen as characteristic area [63]. For subsonic flight at Mach 0.85 at 14000 m altitude, the determined aircraft drag is approximately 10% lower than the thrust that can be provided by two appropriate aero engines, e.g. the Rolls-Royce Pearl 15, at that altitude [36].
Aircraft configurations with two and three engines are investigated respectively. While most subsonic business jets use two engines, some supersonic concepts, e.g. the Aerion AS2 for flight speeds up to Mach 1.4, utilise three engines [64].
The actual drag coefficient c_D has a high influence on the achievable benefit of variable inlet concerning range R, compare Figure 8, and fuel consumption $\dot{m}_{fuel}$, compare Figure 9. The application of variable inlets at Mach 0.95 on an aircraft with two engines and a reasonable c_D-value of 0.025 leads to a range benefit of over 5%. Utilising variable inlets at Mach 1.6 on an aircraft with three engines and a reasonable c_D-value of 0.035 results in a potential range benefit of about 35%. The benefit of using variable inlets instead of fixed inlets increases with the number of engines and with the general reduction of aircraft drag.

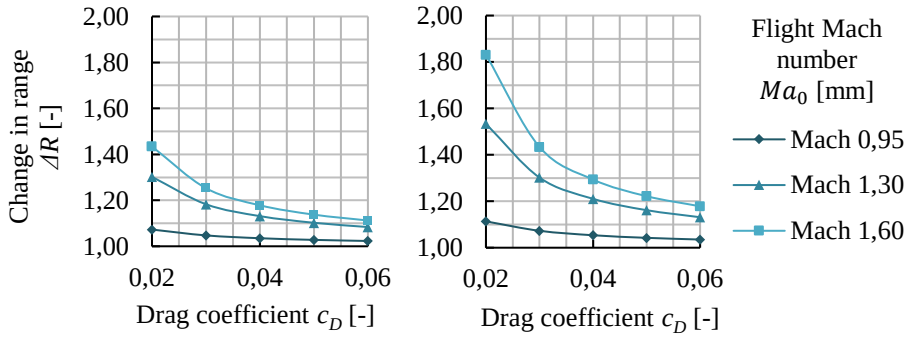

Figure 8: Dependency of achievable range benefit of variable inlets from aircraft drag coefficient and flight Mach number for configurations with two (left) and three (right) engines

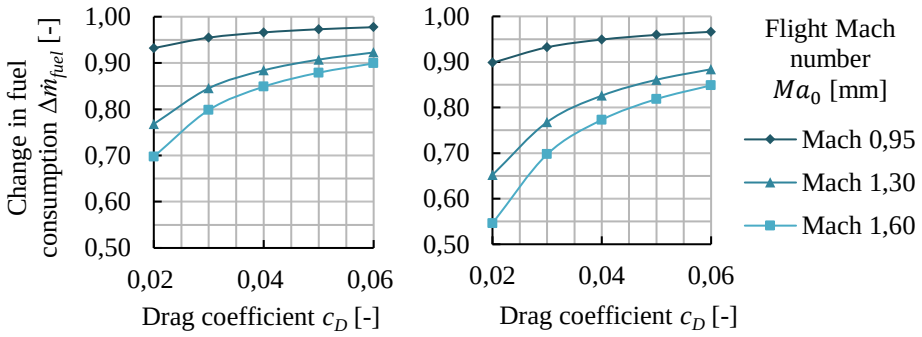

Figure 9: Dependency of achievable fuel consumption benefit of variable inlets from aircraft drag coefficient and flight Mach number for configurations with two (left) and three (right) engines

However, the variable inlet requires an actuation system and is longer than the reference, resulting in additional weight. This additional weight of an aircraft with variable inlets compared to aircraft with conventional inlets has to be considered, as it reduces either the payload or carried fuel weight, and hence the achievable range. The influence of this weight increase is determined by means of Equation (9). For the maximum take-off weight $m_{to,max}$, a value of 47000 kg is selected, which is comparable to aircraft like the Gulfstream G650ER or the Bombardier Global 6500 [41], [38]. For the subsonic flight speeds of Mach 0.85 and 0.95 a c_D-value of 0.025 is selected and for the supersonic speed of Mach 1.3 and 1.6 a c_D-value of 0.035. For a subsonic aircraft for a flight speed of Mach 0.95 and with two engines, a range benefit exists up to an additional overall mass of about 1000 kg, compare Figure 10. This represents an additional weight of 500 kg for each variable inlet. Potential variable inlet concepts should be able to undercut this weight value without difficulties. Supersonic aircraft for a flight speed of Mach 1.6 with three engines would still achieve a range benefit of over 20% for this weight.

DOI: 10.13009/EUCASS2019-314

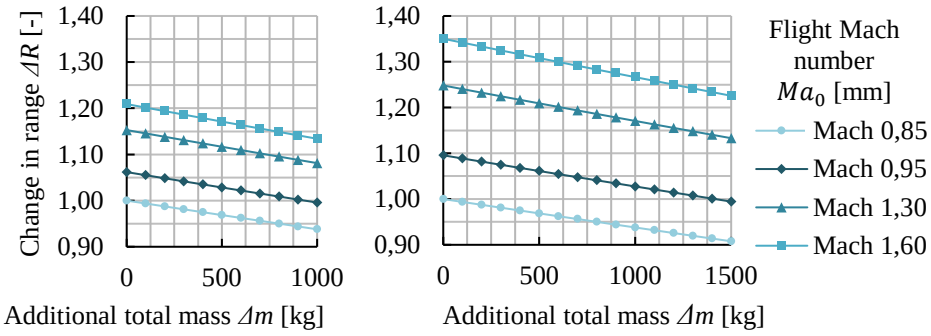

Figure 10: Dependency of achievable range benefit from additional overall mass and flight Mach number for configurations with two (left) and three (right) engines and variable inlets

5. Conclusions

The challenges in inlet design within a concept study for variable pitot inlets in transonic and supersonic civil aviation, as well as relevant geometric parameters and aerodynamic evaluation criteria of inlets have been presented. An approach for a parametric design study has been introduced and implemented. The described approach enables a fast and economical determination of suitable inlet geometries. These geometries are verified by a respective detailed analysis. Their potential benefit regarding range compared to the reference geometry is identified. The presented results can be used as benchmarks; however, additional analyses and tests are recommended. The achievable result quality of the present approach is sufficient for a preliminary investigation and allows an economic identification of ideal inlet geometries for different cruise flight conditions.

The ideal geometries in terms of drag, pressure recovery and flow uniformity, as well as kinematic feasibility have been compared with a rigid commercial geometry. This geometry represents the standard trade-off design of an inlet for an aircraft with a design cruise speed of Mach 0.85. The comparison of the identified geometries with the reference reveals a significant drag reduction at the investigated flight speeds of Mach 0.95, 1.3 and 1.6.

While the drag reduction potentially leads to decreased fuel consumption and increased flight range, the application of variable inlet systems entails additional weight and complexity, as a variable inlet would require an actuation system and utilise a longer inlet. However, by means of a simplified Breguet range equation, the benefit of using variable pitot inlets has been determined. For a conservative additional weight of 500 kg per variable inlet, the range benefit nearly disappears for subsonic applications up to Mach 0.95. On the other hand, a range benefit of over 20% remains for supersonic applications at Mach 1.6.

Following this work, kinematic concepts for circular inlets, which can set the determined ideal geometries, are developed, selected, designed and tested by means of a systems engineering approach with ARP safety considerations [19], [20], [21], [22]. Subsequently, the remaining range benefit after considering additional weight, complexity and potential aerodynamic steps and gaps of the variable system can be determined. This way, the most suitable variable inlet concept can be identified. Concluding, the technology of circular variable pitot inlets for supersonic transport aircraft could be enabled and be a way to achieve the ambitious ecological, safety and economic goals for future civil aviation.

References

[1] European Commission, *Flightpath 2050: Europe's vision for aviation*. Luxembourg: Publ. Off. of the Europ. Union, 2011.

[2] R. W. Luidens, N. O. Stockman, and J. H. Diedrich, *An Approach to Optimum Subsonic Inlet Design*. New York, NY: ASME, 1979.

[3] A. Pierluissi, C. Smith, and D. Bevis, “Intake Lip Design System for Gas Turbine Engines for Subsonic Applications,” in *49th AIAA Aerospace Sciences Meeting*, Orlando, Florida, 2011.

[4] M. Albert and D. Bestle, “Aerodynamic Design Optimization of Nacelle and Intake,” in *Volume 2: Aircraft Engine; Coal, Biomass and Alternative Fuels; Cycle Innovations*, San Antonio, Texas, USA, 2013, V002T01A014.

[5] M. Albert and D. Bestle, “Automatic Design Evaluation of Nacelle Geometry Using 3D-CFD,” in *15th AIAA/ISSMO Multidisciplinary Analysis and Optimization Conference*, Atlanta, GA, 2014.

[6] R. Schnell and J. Corroyer, “Coupled Fan and Intake Design Optimization for Installed UHBR-Engines with Ultra-Short Nacelles,” *ISABE*, 2015.

DOI: 10.13009/EUCASS2019-314

[7] H. Baier, *Morphelle - Project Final Report: Morphing Enabling Technologies for Propulsion System Nacelles*. Munich, Germany, 2015.
[8] S. Kondor and M. Moore, *Experimental Investigation of a Morphing Nacelle Ducted Fan*. Smyrna, GA, 2004.
[9] U. Kling *et al.*, "Shape adaptive technology for aircraft engine nacelle inlets," *Proc. of the Royal Aeronautical Society's 5th Aircraft Structural Design Conference*, 2016.
[10] L. da Rocha-Schmidt, A. Hermanutz, and H. Baier, "Progress Towards Adaptive Aircraft Engine Nacelles," *Proc. of the 29th Congress of the International Council of the Aeronautical Sciences*, 2014.
[11] N. G. Ozdemir *et al.*, "Morphing nacelle inlet lip with pneumatic actuators and a flexible nano composite sandwich panel," *Smart Mater. Struct.*, vol. 24, no. 12, p. 125018, 2015.
[12] D. Grasselt, K. Höschler, and S. Kazula, "A Design Approach for a Coupled Actuator System for Variable Nozzles and Thrust Reverser of Aero Engines," *Proc. of ISABE*, 2017.
[13] H. Smith, "A review of supersonic business jet design Issues," *Aeronaut. j.*, vol. 111, no. 1126, pp. 761–776, https://www.cambridge.org/core/services/aop-cambridge-core/content/view/S0001924000001883, 2007.
[14] M. Hans-Reichel, "Subsonic versus Supersonic Business Jets: Full Concept Comparison considering Technical, Environmental and Economic Aspects," Master Thesis, Wildau Institute of Technology, University of Applied Science, Wildau, 2011.
[15] J. W. Slater, "Methodology for the Design of Streamline-Traced External-Compression Supersonic Inlets," in *50th AIAA/ASME/SAE/ASEE Joint Propulsion Conference*, Cleveland, OH, 2014.
[16] J. Seddon and E. L. Goldsmith, *Intake aerodynamics*, 2nd ed. Reston, Va: American Institute of Aeronautics and Astronautics, 1999.
[17] S. Farokhi, *Aircraft propulsion*. Chichester, West Sussex, United Kingdom: Wiley, 2014.
[18] Federal Aviation Administration, *Fact Sheet – Supersonic Flight.* [Online] Available: https://www.faa.gov/news/fact_sheets/news_story.cfm?newsId=22754. Accessed on: Feb. 22 2019.
[19] S. Kazula and K. Höschler, "A Systems Engineering Approach to Variable Intakes for Civil Aviation," (Eng), *Proceedings of the 7th European Conference for Aeronautics and Space Sciences (Eucass), Milan, Italy*, 2017.
[20] S. Kazula, D. Grasselt, M. Mischke, and K. Höschler, "Preliminary safety assessment of circular variable nacelle inlet concepts for aero engines in civil aviation," in *A Balkema book, Safety and reliability - safe societies in a changing world: Proceedings of the 28th International European Safety and Reliability Conference (ESREL 2018), Trondheim, Norway, 17-21 June 2018*, S. Haugen, A. Barros, C. van Gulijk, T. Kongsvik, and J. E. Vinnem, Eds., Boca Raton, London, New York, Leiden: CRC Press, Taylor et Francis Group, 2018, pp. 2459–2467.
[21] S. Kazula, D. Grasselt, and K. Höschler, "Common Cause Analysis of Circular Variable Nacelle Inlet Concepts for Aero Engines in Civil Aviation," in *IRF2018: Proceedings of the 6th International Conference on Integrity-Reliability-Failure : (Lisbon/Portugal, 22-26 July 2018)*, J. F. Silva Gomes and S. A. Meguid, Eds., Porto: FEUP-INEGI, 2018.
[22] S. Kazula and K. Höschler, "Ice detection and protection systems for circular variable nacelle inlet concepts," *Proceedings of the Deutscher Luft- und Raumfahrtkongress 2018, Friedrichshafen, Germany*, 2018.
[23] S. Kazula and K. Höschler, "A systems engineering approach to variable intakes for civil aviation," *Proceedings of the Institution of Mechanical Engineers, Part G: Journal of Aerospace Engineering*, 095441001983690, 2019.
[24] J. D. Mattingly, *Elements of Propulsion: Gas Turbines and Rockets*. Reston ,VA: American Institute of Aeronautics and Astronautics, 2006.
[25] Rolls-Royce plc., *The jet engine*. Chichester, West Sussex, United Kingdom: Wiley, 2015.
[26] H. Rick, *Gasturbinen und Flugantriebe: Grundlagen, Betriebsverhalten und Simulation*. Berlin, Germany: Springer, 2013.
[27] B. MacIsaac and R. Langton, *Gas Turbine Propulsion Systems*, 1st ed. Chichester, West Sussex, United Kingdom: Wiley, 2011.
[28] EASA, *CS-25: Certification Specifications and Acceptable Means of Compliance for Large Aeroplanes, Amendment 18*, 2016.
[29] J. Albers and E. Felderman, "Boundary-layer Analysis of Subsonic Inlet Diffuser Geometries for Engine Nacelles," *NASA Technical Note D-7520*, 1974.
[30] W. J. G. Bräunling, *Flugzeugtriebwerke: Grundlagen, Aero-Thermodynamik, ideale und reale Kreisprozesse, thermische Turbomaschinen, Komponenten, Emissionen und Systeme*, 4th ed. Berlin, Germany: Springer Vieweg, 2015.
[31] N. A. Cumpsty, *Compressor aerodynamics*. Harlow, Essex: Longman, 1998.
[32] G. C. Oates, Ed., *Aircraft propulsion systems technology and design*. Washington, DC: American Institute of Aeronautics and Astronautics, 1989.
[33] P. M. Sforza, *Theory of aerospace propulsion*. Oxford, United Kingdom, Cambridge, MA, United States: Butterworth-Heinemann, 2017.

DOI: 10.13009/EUCASS2019-314

[34] A. K. Kundu, *Aircraft design*. Cambridge: Cambridge University Press, 2010.
[35] B. Kulfan and J. Bussoletti, “"Fundamental" Parameteric Geometry Representations for Aircraft Component Shapes,” in *Multidisciplinary Analysis Optimization Conferences: 11th AIAA/ISSMO Multidisciplinary Analysis and Optimization Conference*, Portsmouth, Virginia, 2006, p. 71.
[36] Rolls-Royce Plc, *Pearl 15.* [Online] Available: https://www.rolls-royce.com/products-and-services/civil-aerospace/business-aviation/pearl-15.aspx#/. Accessed on: Feb. 22 2019.
[37] S. Kazula, M. Wöllner, D. Grasselt, and K. Höschler, “Parametric design and aero-dynamic analysis of circular variable aero engine inlets for transonic and supersonic civil aviation,” *Proc. of ISABE*, 2019, in press.
[38] Bombardier, *Global 6500.* [Online] Available: https://businessaircraft.bombardier.com/en/aircraft/global-6500. Accessed on: Feb. 22 2019.
[39] EASA, *Type-Certificate Data Sheet for BR700-710 engines*, 2018.
[40] Department of Defence of the United States of America, *MIL-HDBK-310: Military Handbook: Global Climatic Data for Developing Military Products*, 1997.
[41] Gulfstream, *The Gulfstream G650ER.* [Online] Available: http://www.gulfstream.com/aircraft/gulfstream-g650er. Accessed on: Feb. 22 2019.
[42] E. Laurien and H. Oertel, *Numerische Strömungsmechanik*. Wiesbaden: Springer Fachmedien Wiesbaden, 2013.
[43] D. Surek and S. Stempin, *Technische Strömungsmechanik*. Wiesbaden: Springer Fachmedien Wiesbaden, 2014.
[44] R. M. Cummings, W. H. Mason, S. A. Morton, and D. R. McDaniel, *Applied Computational Aerodynamics*: Cambridge University Press, 2018.
[45] D. D. Chao and C. P. van Dam, “Wing Drag Prediction and Decomposition,” *Journal of Aircraft*, vol. 43, no. 1, pp. 82–90, 2006.
[46] C. P. van Dam, “Recent experience with different methods of drag prediction,” *Progress in Aerospace Sciences*, vol. 35, no. 8, pp. 751–798, 1999.
[47] H. Schlichting, K. Gersten, and E. Krause, *Grenzschicht-Theorie: Mit 22 Tabellen*, 10th ed. Berlin, Heidelberg: Springer-Verlag Berlin Heidelberg, 2006.
[48] S. Lecheler, *Numerische Strömungsberechnung*, 4th ed. Wiesbaden: Springer Vieweg, 2018.
[49] ANSYS Inc., *ANSYS Fluent Theory Guide: Release 18.2*. Canonsburg, PA, United States, 2017.
[50] F. R. Menter, “Two-equation eddy-viscosity turbulence models for engineering applications,” *AIAA Journal*, vol. 32, no. 8, pp. 1598–1605, 1994.
[51] ANSYS Inc., *ANSYS Fluent User's Guide: Release 18.2*. Canonsburg, PA, United States, 2017.
[52] J. P. Fielding, *Introduction to aircraft design*. New York, NY: Cambridge University Press, 2017.
[53] M. Robinson, D. G. MacManus, and C. Sheaf, “Aspects of aero-engine nacelle drag,” *Proceedings of the Institution of Mechanical Engineers, Part G: Journal of Aerospace Engineering*, vol. 138, 095441001876557, 2018.
[54] J. A. C. Ambrosio, *Advanced Design of Mechanical Systems: From Analysis to Optimization*, 1st ed. s.l.: Springer Verlag Wien, 2009.
[55] ANSYS Inc., *DesignXplorer User's Guide: Release 18.2*. Canonsburg, PA, United States, 2017.
[56] M. Papageorgiou, M. Leibold, and M. Buss, *Optimierung*. Berlin, Heidelberg: Springer Berlin Heidelberg, 2015.
[57] S. Kazula, M. Wöllner, D. Grasselt, and K. Höschler, “Parametric Design Study on Aerodynamic Characteristics of Variable Pitot Inlets for Transonic and Supersonic Civil Aviation,” *Proc. of EASN*, 2019, in prep.
[58] A. Sóbester, “Tradeoffs in Jet Inlet Design: A Historical Perspective: A Historical Perspective,” *Journal of Aircraft*, vol. 44, no. 3, pp. 705–717, 2007.
[59] S. Kazula, B. Rich, K. Höschler, and R. Woll, “Awakening the Interest of High School Pupils in Science, Technology, Engineering and Mathematics Studies and Careers through Scientific Projects,” in *2018 IEEE International Conference on Teaching, Assessment, and Learning for Engineering (TALE)*, Wollongong, NSW, 2018, pp. 259–265.
[60] A. Filippone, “Data and performances of selected aircraft and rotorcraft,” *Progress in Aerospace Sciences*, vol. 36, no. 8, pp. 629–654, 2000.
[61] A. K. Kundu, D. Riordan, and M. Price, *Theory and practice of aircraft performance*. Place of publication not identified: Wiley, 2016.
[62] NASA, *The Drag Coefficient.* [Online] Available: https://www.grc.nasa.gov/www/k-12/airplane/dragco.html. Accessed on: Feb. 22 2019.
[63] Aviation Week, *Gulfstream G650.* [Online] Available: https://aviationweek.com/business-aviation/gulfstream-g650. Accessed on: Feb. 22 2019.
[64] Aerion Supersonic, *Aerion & Boeing Take the Fast Lane.* [Online] Available: https://www.aerionsupersonic.com. Accessed on: Feb. 22 2019.